Available online at www.sciencedirect.com
SCIENCE DIRECT
Thermochimica Acta 441 (2006) 116–123
thermochimica acta
www.elsevier.com/locate/tca

Thermotropic phase behavior of long-chain alkylammonium-alkylcarbamates

Tomáš Holas, Jarmila Zbytovská, Kateřina Vávrová *, Pavel Berka, Michaela Mádlová, Jana Klimentová, Alexandr Hrabálek

Faculty of Pharmacy, Charles University, Heyrovského 1203, 50005 Hradec Králové, Czech Republic

Received 26 July 2005; received in revised form 6 December 2005; accepted 11 December 2005

Abstract

A series of alkylammonium-alkylcarbamates with different chain length including transdermal permeation enhancer Transkarbam 12 have been prepared and characterized by differential scanning calorimetry (DSC), thermogravimetric analysis (TGA), temperature-dependent Fourier transform infrared spectroscopy (FTIR) and temperature-dependent X-ray powder diffraction. Four transitions have been observed including solid–solid transition (I), melting (II), decomposition of the carbamate salt (III) and boiling of the released amine (IV). The first transition was connected with rearrangement of the hydrocarbon chain packing and unusual shift of symmetric CH_2 stretching vibration in the IR spectra to lower wavenumbers indicated increase of conformational order. The second transition represented melting of the molecule and the third one was attributed to the decomposition of the carbamate salt into two amine molecules and carbon dioxide as evidenced by combination of DSC and TGA curves.

Keywords: Alkylammonium-alkylcarbamates; DSC; TGA; FTIR; Carbon dioxide

1. Introduction

Alkylammonium-alkylcarbamates (AAACs) are of a great importance in biology and industrial applications. Trapping of CO_2 by an amine is valuable for CO_2 removal in various industrial processes such as greenhouse gas control, industrial synthesis [1] and natural gas purification [2]. NASA is currently using a solid amine sorbent for CO_2 removal in space shuttle applications [3]. Carbamates of long-chain aliphatic amines are known to gel a variety of organic liquids [4]. A reversible reaction of CO_2 with fluorescently active amine in polar aprotic solvent rapidly yields carbamic acid salt, which significantly enhances its fluorescence. Such CO_2 sensors have been proposed to be useful in anesthesiology [5].

A series of experiments have been published recently dealing with the chemistry of carbamates at metal centers, i.e. the coordination of CO_2 [6]. Various coordination modes of the carbamate ligands have been reported that could display rich coordination chemistry [7]. The fixation of CO_2 and its transfer to the organic substrates in the Calvin cycle is also initiated by the formation of the metal carbamate complex [8].

We have previously reported a novel group of transdermal permeation enhancers based on AAACs, particularly 5-(dodecyloxycarbonyl)pentylammonium-5-(dodecyloxycarbonyl)pentylcarbamate (Transkarbam 12, T12) [9,10]. The substance enhanced skin transport of drugs with a wide spectrum of physicochemical properties, displayed low toxicity and no dermal irritability. Moreover, an in vitro evaluation showed biodegradability of the compound. One of the hypotheses of the mechanism of action of the carbamate enhancers is a CO_2 release in the intercellular stratum corneum lipid lamellae.

AAACs are formed by reacting CO_2 with two equivalents of a variety of primary and secondary amines, except in case of steric hindrance [11] (Scheme 1). The reaction proceeds both with neat amine and in solution. In aqueous solutions, maximum carbamate formation is observed at pH values corresponding to the p*K*a of the ammonium groups, e.g. 9–10 in the case of the α-amino alkyl groups [12]. The extent to which the position of equilibrium shifts in these thermodynamically driven reactions depends upon the type of amine, its concentration, the pressure

* Corresponding author. Tel.: +420 495 067497; fax: +420 495 514330.
E-mail address: katerina.vavrova@faf.cuni.cz (K. Vávrová).

0040-6031/$ – see front matter © 2005 Elsevier B.V. All rights reserved.
doi:10.1016/j.tca.2005.12.012

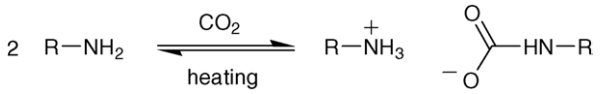

Scheme 1. Synthesis and decomposition of alkylammonium-alkylcarbamates.

of CO_2 and temperature. Several reports on the preparation of crystalline alkylcarbamic acids at low temperatures have been published as well [13]. AAACs are usually crystalline compounds stable at neutral and weakly basic pH levels; however, AAACs with short chains are hygroscopic and unstable. The reaction is reversible by heating or in an acidic environment. In strongly basic solutions, carbamates are readily decomposed to form an alkylammonium-carbonate [2,14].

AAACs formation and breakdown and their equilibria in solutions have been extensively studied [2,15]; however, little attention has been paid to the thermotropic phase behavior and the decomposition of these compounds in a solid state [4,16–18]. We aimed to study the thermotropic phase behavior of a series of model long-chain AAACs, and the permeation enhancer T12. The methods used in this work include differential scanning calorimetry (DSC), thermogravimetric analysis (TGA), temperature-dependent Fourier transform infrared spectroscopy (FTIR) and temperature-dependent X-ray powder diffraction.

2. Experimental

2.1. Synthesis

All chemicals were purchased from Sigma–Aldrich (Darmstadt, Germany). Transkarbam 12 was prepared as described previously [19]. ^{1}H and ^{13}C NMR spectra were measured on a Varian Mercury-Vx BB 300 instrument, operating at 300 MHz for ^{1}H and 75 MHz for ^{13}C. The NMR spectra were recorded in $CDCl_3$ solution with five drops of triethylamine (TEA) to neutralize the trace amounts of deuterons present in $CDCl_3$ that would cause carbamate decomposition. In ^{13}C NMR spectra, a signal of the carbamate carbonyl appeared at 163.4 ppm. The ^{1}H NMR spectrum showed two different signals corresponding to two different α-methylene hydrogens. The elemental analyses (C, H and N) were performed on a Fisons EA 1110 CHNS-O elemental analyzer. Melting points were measured on a Kofler apparatus at 4 °C/min and were uncorrected.

General procedure for the preparation of AAACs: the pertinent amine of 10 mmol was dissolved in 200 ml dry diethyl ether and dry CO_2 was slowly introduced into the mixture for 20 min. The process of crystallization started after several seconds, when the solution began to thin. The crystalline product was filtered off using dense filter paper and dried over P_4O_{10} for 2 h.

To investigate the possible influence of a solvent, $C8CO_2$ was also prepared from acetone, hexane, toluene and water solution. In case of the aqueous solution, the carbamate was prepared from octylammonium-chloride and Na_2CO_3.

2.1.1. Octylammonium-octylcarbamate ($C8CO_2$)

White crystals; yield: quant.; mp 71–81 °C; (Found: C, 67.1; H, 12.55; N, 9.1. Calc. for $C_{17}H_{38}N_2O_2$: C, 67.5; H, 12.7; N, 9.3%); ν_{max}(nujol)/cm^{-1} 3331, 2170, 1652, 1574, 1320, 1306 and 1151; δ_H(300 MHz; $CDCl_3$ + TEA) 7.76 (3H, br s, NH_3^+), 4.50 (1H, br s, N*H*), 3.00 (2H, t, *J* 6.9, CH_2NH), 2.70 (2H, t, *J* 7.7, CH_2NH_3^+), 1.47–1.62 (2H, m, CH_2), 1.34–1.47 (2H, m, CH_2), 1.14–1.34 (20H, m, 10 × CH_2), 0.86 (6H, t, *J* 6.8, 2 × *CH*$_3$); δ_C(75 MHz; $CDCl_3$ + TEA) 163.4, 41.8, 40.6, 31.8, 30.7, 29.3, 29.3, 26.8, 22.6, 14.1.

2.1.2. Nonylammonium-nonylcarbamate ($C9CO_2$)

White crystals; yield: quant.; mp 70–82 °C; (Found: C, 68.7; H, 12.9; N, 8.5. Calc. for $C_{19}H_{42}N_2O_2$: C, 69.1; H, 12.8; N, 8.5%); ν_{max}(nujol)/cm^{-1} 3331, 2173, 1651, 1574, 1314, 1151, 818.

2.1.3. Decylammonium-decylcarbamate ($C10CO_2$)

White crystals; yield: quant.; mp 72–83 °C; (Found: C, 70.7; H, 13.0; N, 8.0. Calc. for $C_{21}H_{46}N_2O_2$ C, 70.3; H, 12.9; N, 7.8%); ν_{max}(nujol)/cm^{-1} 3331, 2165, 1650, 1567, 1321, 1305, 1152, 817.

2.1.4. Undecylammonium-undecylcarbamate ($C11CO_2$)

White crystals; yield: quant.; mp 75–83 °C; (Found: C, 71.0; H, 13.2; N, 7.3. Calc. for $C_{23}H_{50}N_2O_2$ C, 71.45; H, 13.0; N, 7.25%); ν_{max}(nujol)/cm^{-1} 3331, 2169, 1651, 1568, 1315, 1151, 817.

2.1.5. Dodecylammonium-dodecylcarbamate ($C12CO_2$)

White crystals; yield: quant.; mp 73–83 °C; (Found: C, 72.1; H, 13.4; N, 6.85. Calc. for $C_{25}H_{54}N_2O_2$ C, 72.4; H, 13.1; N, 6.75%); ν_{max}(nujol)/cm^{-1} 3331, 2170, 1650, 1567, 1315, 1151, 817.

2.1.6. Hexadecylammonium-hexadecylcarbamate ($C16CO_2$)

White crystals; yield: quant.; mp 82–87 °C; (Found: C, 74.85; H, 13.4; N, 5.4. Calc. for $C_{33}H_{70}N_2O_2$ C, 75.2; H, 13.4; N, 5.3%); ν_{max}(nujol)/cm^{-1} 3331, 2152, 1647, 1657, 1314, 1157, 816.

2.2. DSC

The thermograms were recorded in the temperature range of −90 to 200 °C using a Netzsch DSC 200PC instrument (NETZSCH-Gerätebau GmbH, Selb/Bayern, Germany) at a scan rate of 5 and 1 °C/min, respectively. Samples of ca. 4 mg were placed in an aluminum crucible with a perforated lid for the release of rising gas. The "sample + correction" measurement was used and N_2 was applied as the purge gas at 20 ml/min. The phase transitions were characterized by the onset or end temperatures, which were determined with an accuracy of 0.8% by exploration of the most rapid increase in the excess heat capacity curve using Netzsch Proteus, Thermal Analysis software, Version 4.3. The enthalpy change (ΔH) was obtained by integrating the area under the transition peak with an accuracy of 0.83%. The enthalpy of overlapped peaks was determined from the area under the fitted peaks using the PeakFit software v.4.

2.3. TGA

The thermogravimetric behavior of the AAACs was analyzed using a Stanton Redcroft TG 750 instrument (England). A sample of 6 mg was examined in an inert atmosphere at a heating rate of 5 °C/min.

2.4. FTIR spectroscopy

The temperature-dependent IR spectra were collected on a FTIR NICOLET NEXUS EURO spectrometer (Mid-IR), equipped with a DTGS/KBr detector and XT-KBr beamspliter. The thermostat (Optistat CF-V/Oxford Instruments, KSR5 windows) was equipped with a temperature control accessory (temperature regulator = ITC 503, LabView 6.1/National Instruments) and membrane vacuum pump (allowed vacuum about 0.3 kPa). The temperature dependence was studied in the range of 25–130 °C in 1 °C/min increments. The background was acquired against empty shutter at room temperature. The spectra were recorded with 64 scans (77 s) automatically every second minut of heating with the resolutions of 2 cm^{-1}. To obtain transparent KBr disks, it was necessary to add the substance of $C8CO_2$ (0.7 mg) to the ground KBr (300 mg) without mixing the compounds together in a molecular mill. For examination of the overlapped peaks in the region of 1680–1525 cm^{-1} PeakFit software v.4 was used. The temperature dependence of the band intensity was interpreted according to the reference band at 2800–3000 cm^{-1}.

2.5. X-ray diffraction

The diffractograms were measured in the reflection mode on the Bruker D8 Advance (Bruker Optik, Ettlingen, Germany) diffractometer operating with Cu Kα1 radiation (λ = 1.5418 Å, 40 kV, 30 mA) equipped with a secondary beam monochromator and a scintillation detector. The intensities were recorded in the scattering angle of $0° < 2\vartheta < 35°$. The sample heating was achieved by a current connected Pt strip. The temperature dependence of the X-ray diffraction was studied in 1 °C/min steps. Lamellar spacing was calculated according to the Bragg's law: $d = n\lambda/2\sin\vartheta$, where d is the distance between the two parallel planes (Å), n the diffraction orders, λ the wavelength of the X-ray beam and ϑ is scattering angle.

3. Results

3.1. DSC

The DSC thermogram of $C8CO_2$ recorded at a scan rate of 5 °C/min exhibited four endothermic peaks (Fig. 1). The first transition (I) with the onset/end temperature of 52.5/60.4 °C was accompanied by ΔH = 11.7 kJ/mol. The position of the transition (I) did not change in $C8CO_2$ precipitated from diethyl ether, acetone, hexane, toluene and water, respectively. The second peak (II) at 85.0/91.5 °C was connected with ΔH = 36.0 kJ/mol. The third peak (III) showed, after the peak fit, the same onset value as the peak (II) and the offset at 130 °C. This transition was

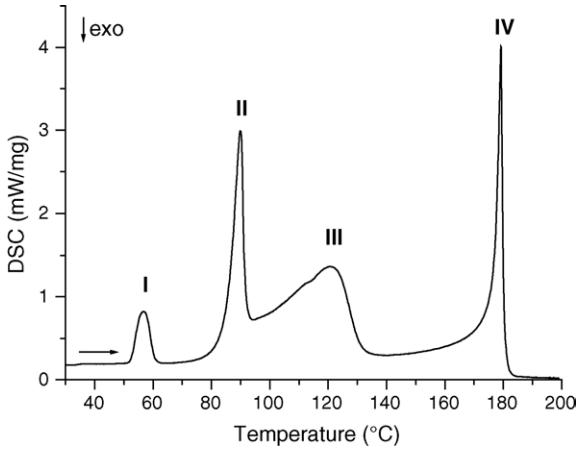

Fig. 1. The DSC curve of $C8CO_2$ at a temperature scan rate of 5 °C/min: heating from room temperature to 200 °C.

associated with ΔH = 118.1 kJ/mol. Overlapping of the peaks (I) and (II) was observed at longer-chain AAACs (see below). The DSC curve of $C8CO_2$ collected at a scan rate of 1 °C/min constitutes the transition (I) with the onset/end temperature of 48.6/53.3 °C, the transition (II) with onset/end temperature of 80.6/85.6 °C and the transition (III) with the same onset value as the peak (II) and the offset at 109 °C (Figs. 9 and 11).

In the second DSC experiment, $C8CO_2$ was heated up to 67 °C, cooled down to 20 °C and then reheated to 100 °C at a scan rate of 5 °C/min (Fig. 2). During the first heating, transition (I) was observed, however, none was detected during cooling. During the second heating up to 100 °C, only the transition (II) was observed; transition (I) was absent.

In the third DSC experiment, the behavior of $C8CO_2$ was examined in a range of temperatures from −90 to 120 °C at a scan rate of 5 °C/min (Fig. 3, Table 1). First, the sample was heated from −90 °C to 67 °C, i.e. over transition (I), and cooled to −90 °C. In contrast to the second experiment, an exothermic peak (Ib) appeared. During second heating to 100 °C, transition (Ib) appeared at 44.8 °C. At cooling to −90 °C and reheating to

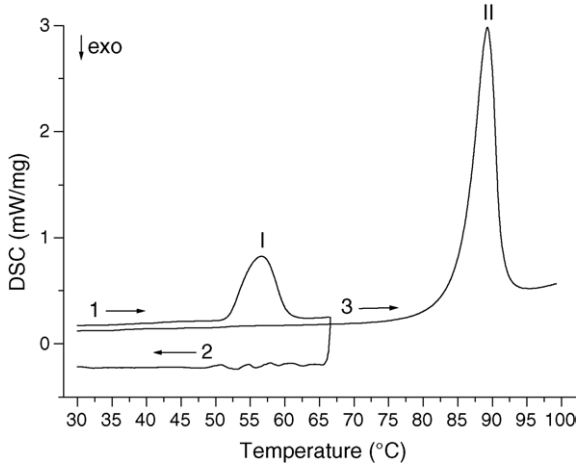

Fig. 2. The DSC curve of $C8CO_2$ at a temperature scan rate of 5 °C/min: (1) heating to 67 °C, (2) cooling to room temperature and (3) second heating to 100 °C.

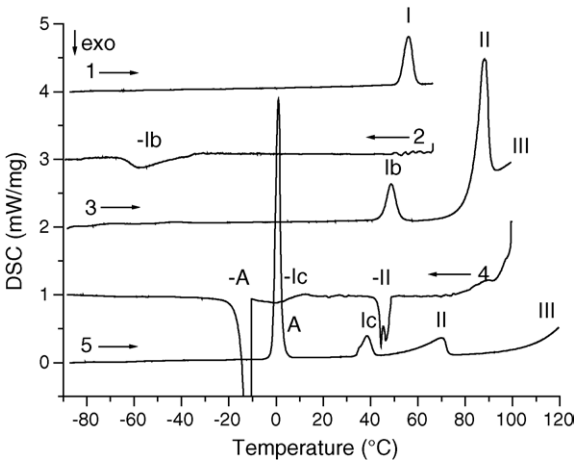

Fig. 3. The DSC curve of $C8CO_2$ at a temperature scan rate of 5 °C/min: (1) heating from −90 to 67 °C, (2) cooling to −90 °C, (3) heating to 100 °C, (4) cooling to −90 °C and (5) heating to 120 °C.

120 °C, transitions of free octylamine -A and A and transitions -Ic and Ic were observed as shown in Fig. 3. The peaks (-Ib), (-II), (-Ic) and (-A) were in enthalpy relation to (Ib), (II), (Ic) and (A), respectively (Table 1). With repeated heating/cooling cycles from −90 °C to 100 °C and back to −90 °C, transitions (II) and (III) shifted to lower temperatures each cycle and finally disappeared, while the position of transition (Ic) was stable.

Fig. 4 describes the relationship between the enthalpy change of the transitions (I), (II) and (III) and the chain length of AAACs at a scan rate of 5 °C/min. While the enthalpy change of the transition (III) was independent of the chain length, the enthalpy change associated with transitions (I) and (II) exhibited a positive linear dependence on the chain length.

Similar DSC experiments were performed for the skin permeation enhancer T12 at a scan rate of 5 °C/min (Fig. 6). During heating, the transition (I) with the onset/end at 49.2/59.1 °C and ΔH = 13.8 kJ/mol, the transition (II) with the onset at 68.5 °C and ΔH = 119.4 kJ/mol, and the transition (III) with the same onset as (II) and ΔH = 108 kJ/mol were observed. No boiling point was detected under 200 °C, because of high molecular weight of the released amino ester. The DSC curve of T12 did not reach the baseline between the transitions (I) and (II), therefore $C8CO_2$

Table 1
Description of the peaks observed in the third DSC experiment

DSC heating/cooling (°C)	Peak	Onset/end (°C)	ΔH (kJ/mol)
1. −90 → 67	(I)	52.5/60.4	11.7
2. 67 → −90	(-Ib)	−30.0/−70.0	−9.9
3. −90 → 100	(Ib)	44.8/52.5	9.9
	(II)	85.0/91.5	36.0
4. 100 → −90	(-II)	41.9/48.5	−9.3
	(-Ic)	8.3/−10.6	−4.8
	(-A)	−10.7/−22.0	−15.4[a]
5. −90 → 120	(A)	−1.4/3.0	15.3[a]
	(Ic)	33.9/41.5	5.1
	(II)	41.9/72.9	9.3

[a] Calculated for free amine.

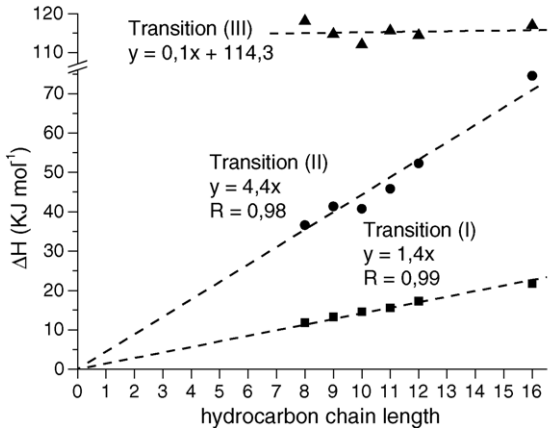

Fig. 4. The dependence of the enthalpy change at transition (I), (II) and (III) on the hydrocarbon chain length of the selected AAACs at a temperature scan rate of 5 °C/min.

proved to be a more valuable tool to study the thermotropic phase behavior of AAACs.

3.2. TGA

In contrast to DSC, TGA uses an open pan for analysis. For the measurement of the weight loss connected with carbon dioxide release, it was necessary to select a carbamate, which decomposes into amine of low volatility. $C8CO_2$, for example, was not suitable because a simultaneous loss of both CO_2 and octylamine was observed. Therefore, $C16CO_2$ was chosen as the model AAAC in order to combine the DSC and TGA results (Fig. 5). Although the three transitions of $C16CO_2$ were overlapped, TGA results confirmed that CO_2 is released from the carbamate not until the end of the third transition (as evidenced by 8.4% loss of weight).

Similar experiments were performed for the permeation enhancer T12 (Fig. 6). The first transition was not accompanied by any weight loss and after the second one, the sample still retained about 99% of its initial weight. The 1% loss could be explained by the beginning of the third transition at the same temperature. Only after transition (III), CO_2 from the T12 molecule

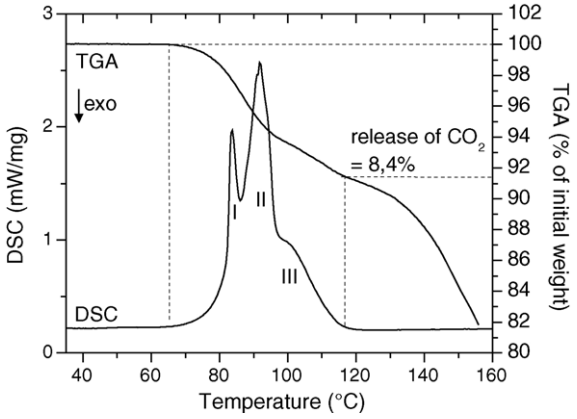

Fig. 5. The DSC and TGA curves of $C16CO_2$ at a temperature scan rate of 5 °C/min: dashed lines represent the release of carbon dioxide from the carbamate structure.

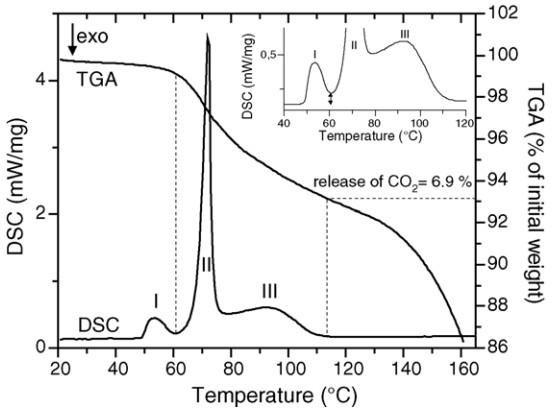

Fig. 6. The combination of DSC and TGA curves of T12 heated from 25 to 160 °C at a temperature scan rate of 5 °C/min. Dashed lines represent the release of carbon dioxide from the carbamate structure. The arrow in inset indicates, that the curve does not reach the baseline between transition (I) and (II) as in the model carbamate $C8CO_2$.

was lost. It confirms that the degradation of the carbamate salt is not connected with transition (I) but (III). Similar dependence of TGA on DSC was also observed in other T12 analogs with different functional groups instead of the ester one [20].

3.3. FTIR spectroscopy

The infrared spectra of $C8CO_2$ measured in KBr at 41, 66 and 100 °C are shown in Fig. 7. The spectrum at 41 °C is consistent with that measured at room temperature, except for the NH vibration as discussed below. Released CO_2 was not observed in the spectra.

3.3.1. Changes in polar head group

3.3.1.1. NH vibration. The band at 3332 cm^{-1} at room temperature was assigned to the NH stretching vibration of the carbamate group [17]. During temperature increase, the position of the band first shifted to 3336 cm^{-1} at 48 °C, and then decreased rapidly to 3324 cm^{-1}. At 56 °C, the wavenumber began to increase again (Fig. 8). However, the intensity of the vibration remained unchanged until transition (II). Afterwards,

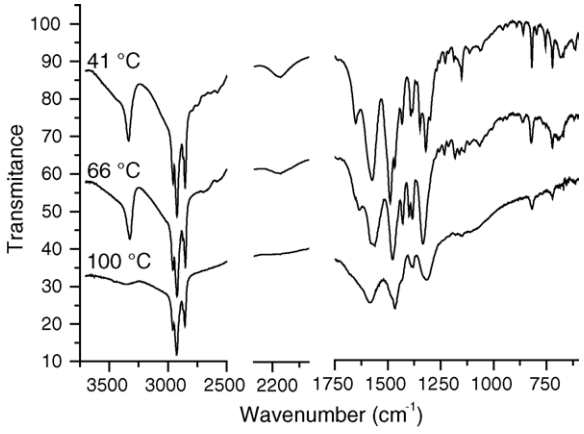

Fig. 7. The infrared spectrum of $C8CO_2$ in KBr tablet at 41, 66 and 100 °C.

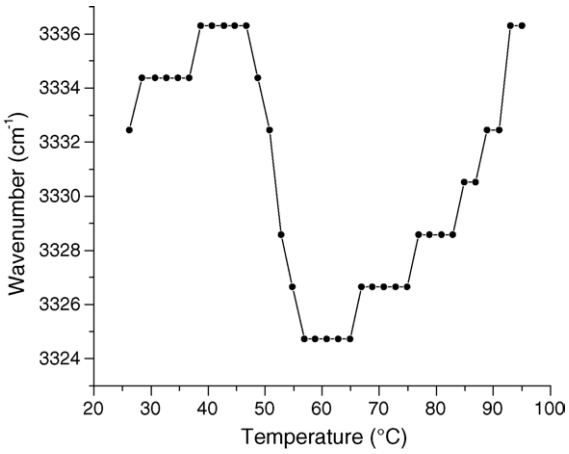

Fig. 8. Temperature dependence of band position of the NH stretching vibration at a temperature scan rate of 1 °C/min.

the intensity started to decrease and the band completely disappeared at 95 °C (Fig. 9).

3.3.1.2. Combination band of RNH_3^+ torsion and antisymmetric RNH_3^+ deformation. The band at 2170 cm^{-1} indicated the presence of ammonium ions [21] because the other RNH_3^+ bands were overlapped by those of NH and amide II. The band position was not temperature-dependent, however, its intensity behaved similarly to the NH vibration (Fig. 9).

3.3.1.3. Amide I and amide II bands. The amide I band at 1652 cm^{-1} does not correspond to pure C=O stretching, it includes C–N stretching and N–H deformation as well [17]. Around 50 °C, the band shifted to lower wavenumbers at 1635 cm^{-1}. At 95 °C, the band completely disappeared (Fig. 9). The band at 1574 cm^{-1} at room temperature was fitted into two bands with maxima at 1598 and 1567 cm^{-1} (Fig. 10). The band at 1567 cm^{-1} could be assigned to the amide II vibration comprising the deformation and the vibration of the whole $NHCOO^-$ group [22]. The band at 1598 cm^{-1} belongs to the antisymmetric deformation of RNH_3^+ [21]. At transition (I), both bands at 1598 and 1567 cm^{-1} shifted to 1584 and 1553 cm^{-1}, respec-

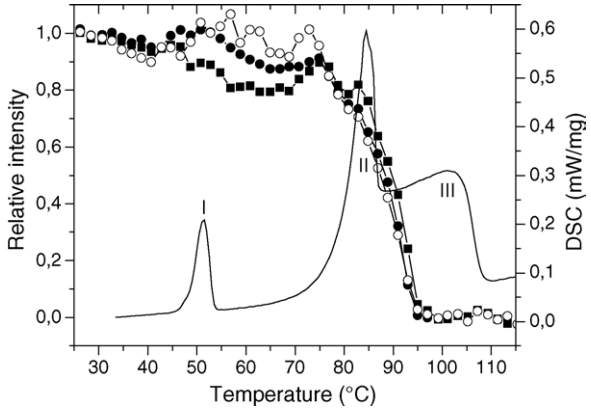

Fig. 9. Relative intensities of NH (open circles), NH_3^+ (filled squares) and amide I bands (filled circles) vs. temperature and the DSC curve of $C8CO_2$ at a temperature scan rate of 1 °C/min.

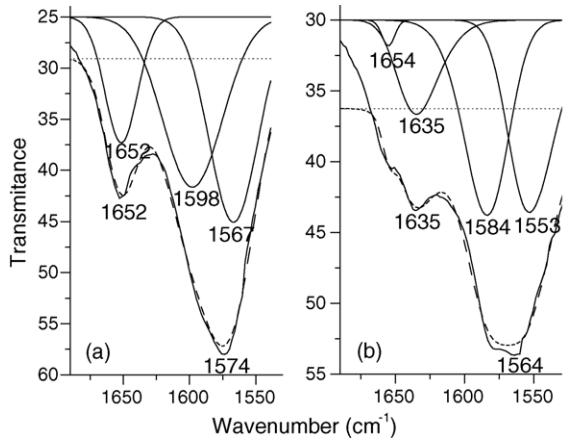

Fig. 10. Temperature dependence of fitted IR spectra in the spectral range from 1680 to 1525 cm^{-1} at 41 °C (a) and at 66 °C (b). Dots are baselines of fitting.

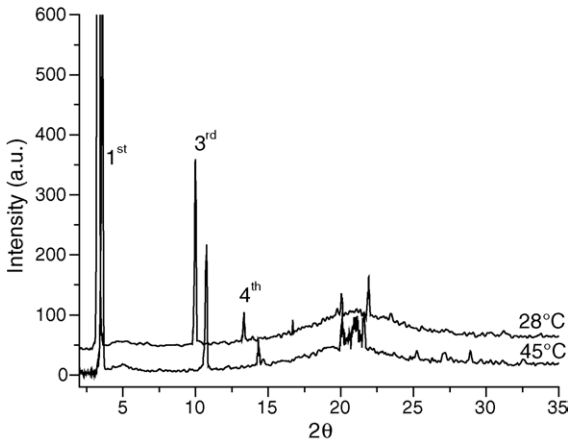

Fig. 12. Temperature dependence of powder diffraction patterns of $C8CO_2$ at a temperature scan rate of 1 °C/min. Diffraction orders are displayed.

tively. Above 100 °C, the bands merged to one broad symmetric band at 1583 cm^{-1} representing the scissoring deformation of NH_2 (Fig. 7).

3.3.2. Changes in hydrocarbon chains

3.3.2.1. CH stretching region. The temperature-dependent shift of the CH_2 stretching band is related to the changes in the *trans*/*gauche* conformation ratio in the hydrocarbon chains. Generally, lower position of the symmetric CH_2 stretching vibration indicates a high content of *trans* conformers [23]. The thermotropic response of the positions is shown in Fig. 11. At room temperature, the antisymmetric $\nu_{as}(CH_2)$ and symmetric $\nu_s(CH_2)$ stretching vibrations were observed at 2924 and 2854 cm^{-1}, respectively. At the transition (I), the position of $\nu_s(CH_2)$ decreased to 2852 cm^{-1} while the asymmetric one remained unchanged. At 80 °C (transition (II)), the positions of $\nu_{as}(CH_2)$ and $\nu_s(CH_2)$ vibrations increased to 2926 and 2854 cm^{-1}, respectively, and the position $\nu_s(CH_2)$ vibration further increased to 2856 cm^{-1} at 91 °C.

3.3.2.2. CH_2 rocking. The CH_2 rocking band is found at 721 cm^{-1}. With increasing temperature, the band remained in the same position. No splitting of the band was observed, which indicates that only one chain is present in a subcell. According to this finding, the hydrocarbon chains can be arranged in a triclinic or hexagonal chain packing [24].

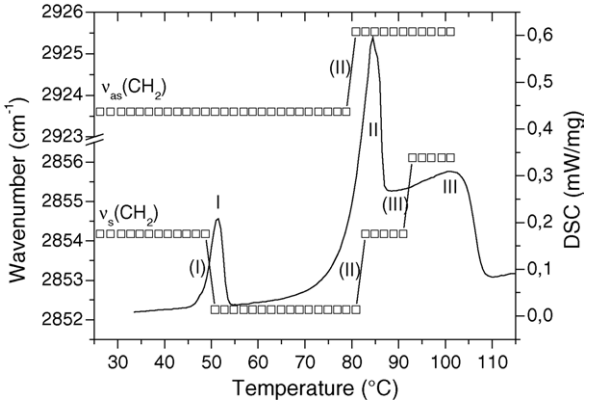

Fig. 11. Band position of the symmetric stretching mode $\nu_s(CH_2)$ and the asymmetric stretching mode $\nu_{as}(CH_2)$ vs. temperature for $C8CO_2$ and the DSC curve of $C8CO_2$ at a temperature scan rate of 1 °C/min.

3.4. X-ray diffraction

The powder diffraction pattern of $C8CO_2$ before the first transition, showed the first, third and fourth diffraction order of a one-dimensional lamellar geometry (Fig. 12). At 20 °C, the phase exhibited a lamellar spacing of 26.61 ± 0.15 Å. During the transition (I) observable already at 45 °C, the lamellar spacing decreased to 24.80 ± 0.10 Å. The wide-angle X-ray diffraction of $C8CO_2$ demonstrated that the transition (I) was connected with the change of the subcell parameters.

4. Discussion

In an attempt to elucidate the phase behavior and consequently the mechanism of action of the skin permeation enhancer T12, the physico-chemical behavior of AAACs has been investigated. Although there are many studies dealing with formation, decomposition and equilibria of AAACs in solutions, their behavior in solid state is not fully understood [4,16–18]. A homology series of C8–C16 AAACs was selected as a representative for the long-chain AAACs with octylamine-derived carbamate salt $C8CO_2$ for most experiments.

The solvents used for preparation of the AAACs had no influence on their phase behavior in a solid state. Although equilibria between free amine, carbamic acid, molecular complex, ammonium carbamate and its dimer occur in solution [15] and are strongly influenced by the nature of the solution, pure AAACs were prepared in this work. This is due the decreased solubility of the long-chain AAACs leading to precipitation from the reaction mixture. The precipitation shifts the reaction equilibrium towards the AAAC and permits isolation of the desired product.

At room temperature, the X-ray powder diffraction indicated that there was only one crystal arrangement with a lamellar

spacing of 26.5 Å, which is in agreement with that of other AAACs [18] According to the $\nu_s(CH_2)$ stretching band position, the hydrocarbon chains were in an ordered structure, with certain proportion of *gauche* conformers. Non-splitting of the CH_2 rocking band suggested that the chains were in triclinic subcell chain packing.

The first transition at about 50 °C represented a solid–solid phase transition. Although the X-ray powder diffraction indicated that the lamellar spacing of $C8CO_2$ decreased to 24.8 Å, the transition was not connected with CO_2 release as evidenced by DSC and TGA experiments. When $C8CO_2$ was heated over the transition (I), cooled and heated again, no free amine was detected (Fig. 2). Furthermore, TGA of $C16CO_2$ and T12 clearly showed that no weight loss occurred during the first transition (Figs. 5 and 6). The shift of the symmetric CH_2 stretching vibration to the lower wavenumbers indicated an increase in the conformational order in the hydrocarbon chains.

A possible explanation of the observations associated with transition (I) is that the crystals of AAACs change the specific packing arrangement of the hydrocarbon chains, particularly the angle between the chains. Regarding that the intercept value of linear regression for the transition (I) is zero (Fig. 4), it could be hypothesized that the energy change of the transition (I) involves rearranging the hydrocarbon chains. Although shifts of NH, amide I and II vibrations to the lower wavenumbers were observed in the IR spectra, the band intensities remained unchanged (Fig. 9). This confirms that the carbamate group was not decomposed at transition (I). The down-shifts in the IR spectra contrasted with the usually observed shifts to higher wavenumbers due to weakening of the hydrogen bonds with temperature increase. According to Fig. 4, there are either no electrostatic changes caused by alteration of the subcell parameters at transition (I) or there are both positive and negative forces that are balanced. A shift of symmetric CH_2 stretching vibrations to lower wavenumbers suggests that this new chain packing is quite stable. Presumably, the change in the polar head could lead to increased chain order. The X-ray diffraction study of T12 demonstrated that transition (I) was connected only with the change in packing arrangement in contrast with $C8CO_2$, where we observed also the change in lamellar spacing. This could be due to presence of ester bond in T12.

The second transition represents melting. The melting of $C8CO_2$ starts at about 80 °C, the process was observed also in the IR spectra. The positions of both CH_2 stretching vibrations shifted to higher wavenumbers, which indicated an increased amount of *gauche* conformers. The enthalpy of the transition (II) was dependent only on the length of the hydrocarbon chain (Fig. 4). Since this transition began together with transition (III), the NH and CO vibrations and the combination vibration of NH_3^+ began to disappear with melting and were no more visible at the end of the transition (III) at about 95 °C (Fig. 9).

The third transition is connected with degradation of the carbamate salt into amine and CO_2 (Figs. 1, 5 and 6). After heating to 100 °C, the carbamate was partially decomposed and free amine evidenced by peak (-A) on cooling and (A) on subsequent heating, respectively (Fig. 3). With repeating of the heating/cooling cycles, the partially released amine could form a eutectic mixture with the residual carbamate, leading to a shift of the second and third transitions to lower temperatures. The significant release of free amine was clearly observed also in the IR spectra (Fig. 8). Above transition (III), the shift of symmetric CH_2 stretching vibration to higher wavenumbers indicated highly disordered hydrocarbon chains typical for liquid phase. The enthalpy of this transition was independent of the hydrocarbon chain length; for the release of CO_2 from various AAACs, energy of approximately 114 kJ/mol was needed (Fig. 4).

The fourth transition of $C8CO_2$ represents boiling of octylamine [25]. In the other carbamates and T12, the fourth transition was not evident, because the boiling points of the pertinent amines were too high.

The above mentioned assignments of the first three transitions correspond well with the enthalpies, because the energy needed for a chemical reaction (decomposition of the carbamate) is generally higher than that for melting and only minimum energy is needed for the change in crystal structure (Fig. 4).

All known stable AAACs are described only as solid structures and not liquids. It is possible that for stabilization of AAACs hydrogen bonds are not sufficient and a certain length of the hydrocarbon chains accompanied by van der Waals interactions is needed. This could explain why some AAACs, e.g. short-chained and branched ones are not possible to isolate at room temperature [20]. Presence of the solvent molecules accompanied by H-bonding interactions stabilizes the AAACs as well [15].

Previously, only two transitions were described in T12 [16]. It was suggested that the first one, with the onset at 53 °C was related to changes in the polar head group and decomposition of the carbamate structure. However, no evidence for CO_2 release was observed, therefore, it was hypothesized that it stays within the molecule bonded with a non-covalent interaction. The second transition was identified as melting accompanied with the release of CO_2. However, the study described the behavior in a temperature range of 40–85 °C and used different heating regimes for DSC and FTIR. In this study, where the same scan rate of 1 °C/min was used for both DSC and FTIR, no disappearance of NH and CO vibrations at the first transition was observed. However, the atypical shifts of symmetric CH_2 stretching vibrations to lower wavenumbers were described during the transition (I) in both experiments. In this study, the carbamate decomposition was firmly attributed to the third transition. The DSC and TGA thermograms of T12 (Fig. 6) were in good correlation with the results obtained for AAACs and the enthalpy of the transition (III) of T12 was in good agreement with that of AAACs (108 and 114 kJ/mol, respectively).

We have previously found that only the ammonium carbamate form, Transkarbam 12, was responsible for the high transdermal permeation-enhancing activity and the pertinent free amine was completely inactive. Moreover, a pH dependence of the enhancing effect was observed suggesting that the most important feature is the carbamate anion and the carbonate is not active [26]. Such chemical structure is completely novel in the group of skin permeation enhancers. The results from this study are important for further studies of the interactions of T12 with the stratum corneum lipids, e.g. miscibility and phase behavior.

5. Conclusion

The thermotropic phase behavior of alkylammonium-alkylcarbamates was studied using a combination of four experimental methods. With increasing temperature, four transitions were observed. The experimental studies provided evidence for the relation of the first transition to changes in crystal structure. The second transition represented the melting of the hydrocarbon chain. The third transition, assigned to the carbamate structure decomposition started simultaneously to the second transition. The fourth transition represented boiling of the liberated amine. It was suggested that a certain hydrocarbon chain is needed to obtain stable alkylammonium-alkylcarbamates.

Acknowledgements

The work was supported by the Ministry of Education of the Czech Republic (grant MSM0021620822). We thank M. Kincl, J. Maixner and J. Ederová for their assistance with the temperature-dependent IR spectra, X-ray powder diffraction and thermogravimetric analysis, respectively.

References

[1] W. McGhee, D. Riley, K. Christ, Y. Pan, B. Parnas, J. Org. Chem. 60 (1995) 2820–2830.
[2] E. Jørgensen, Acta Chem. Scand. 10 (1956) 747–755;
M.B. Jensen, Acta Chem. Scand. 11 (1957) 499–505.
[3] S. Satyapal, T. Filburn, J. Trela, J. Strange, Energy Fuels 15 (2001) 250–255.
[4] M. George, R.G. Weiss, Langmuir 18 (2002) 7124–7135.
[5] E.M. Hampe, D.M. Rudkevich, Chem. Commun. 14 (2002) 1450–1451.
[6] D.B. Dell'Amico, F. Calderazzo, S. Farnocchi, L. Labella, F. Marchetti, Inorg. Chem. Commun. 5 (2002) 848–852;
R. Nomura, Y. Hasegawa, M. Ishimoto, T. Toyosaki, H. Matsuda, J. Org. Chem. 57 (1992) 7339–7342;
K.C. Yang, C.C. Chang, C.S. Yeh, G.H. Lee, S.M. Peng, Organometallics 20 (2001) 126–137;
M.T. Caudle, R.A Nieman, V.G. Young Jr., Inorg. Chem. 40 (2001) 1571–1575.
[7] G.B. Deacon, R.J. Phillips, Coord. Chem. Rev. 33 (1980) 227–250.
[8] D. Walther, M. Ruben, S. Rau, Coord. Chem. Rev. 182 (1999) 67–100.
[9] P. Doležal, A. Hrabálek, V. Semecký, Pharm. Res. 10 (1993) 1015–1019.
[10] A. Hrabálek, P. Doležal, O. Farsa, A. Krebs, A. Kroutil, M. Roman, Z. Šklubalová, US Pat. 6,187,938 (2001).
[11] A.K. Chakraborty, K.B. Bischoff, G. Astarita, J.R. Damewood Jr., J. Am. Chem. Soc. 110 (1988) 6947–6954.
[12] R.U. Lemieux, M.A. Barton, Can. J. Chem. 49 (1971) 767.
[13] M. Aresta, D. Ballivet-Tkatchenko, D.B. Dell'Amico, M.C. Bonnet, D. Boschi, F. Calderazzo, R. Faure, L. Labella, F. Marchetti, Chem. Commun. 13 (2000) 1099–1100;
G.A. Olah, M. Calin, J. Am. Chem. Soc. 90 (1968) 401–404.
[14] A. Jensen, C. Faurholt, Acta Chem. Scand. 6 (1952) 385–394.
[15] U.B. Mioč, S. Ribnikar, Bull. Soc. Chim. Beograd (EN) 43 (1978) 603–612;
U.B. Mioč, S. Ribnikar, Bull. Soc. Chim. Beograd (EN) 44 (1979) 189–194;
K. Masuda, Y. Ito, M. Horiguchi, H. Fujita, Tetrahedron 61 (2005) 213–229;
M. George, R.G. Weiss, Langmuir 19 (2003) 8168–8176.
[16] J. Zbytovská, S. Raudenkolb, S. Wartewig, W. Hübner, W. Rettig, P. Pissis, A. Hrabálek, P. Doležal, R.H.H. Neubert, Chem. Phys. Lipids 129 (2004) 97–109.
[17] E. Carretti, L. Dei, P. Baglioni, R.G. Weiss, J. Am. Chem. Soc. 125 (2003) 5121–5129.
[18] M. George, R.G. Weiss, Langmuir 19 (2003) 1017–1025.
[19] US Pat. 6,187,938 (2001).
[20] T. Holas, Ph.D. Thesis, Charles University in Prague, Faculty of Pharmacy in Hradec Králové, 2006.
[21] M. Horák, D. Papoušek, Infračervená Spektra a Struktura Molekul, Academia, Praha, 1976, p. 246;
M. Horák, D. Papoušek, Software: Spectool for Windows 3.1 Version 1.0, 1976;
K. Nakanishi, T. Goto, M. Ohashi, Bull. Chem. Soc. Jpn. 30 (1957) 403–408.
[22] E. Leibnitz, W. Hager, S. Gipp, P. Bornemann, J. Prakt. Chem. 4 (1959) 217–231.
[23] R.G. Snyder, J.H. Schachtschneider, Spectrochim. Acta 19 (1963) 85–116;
K. Brown, E. Bicknell-Brown, M. Ladjadj, J. Phys. Chem. 91 (1987) 3436–3442.
[24] M. Kobayashi, F. Kaneko, K. Sato, M. Suzuki, J. Phys. Chem. 90 (1986) 6371–6378.
[25] www.sigmaaldrich.com.
[26] A. Hrabálek, P. Doležal, K. Vávrová, J. Zbytovská, T. Holas, J. Klimentová, J. Novotný, Pharm. Res. (2006), in press.